Georgia Institute of Technology

The George W. Woodruff School of Mechanical Engineering
Nuclear & Radiological Engineering/Medical Physics Program

Ph.D. Qualifier Exam

Fall Semester 2007

_______________ Your ID Code

Radiation Detection & Protection (Day 3)

Instructions

1. Use a separate page for each answer sheet (no front to back answers).
2. The question number should be shown on each answer sheet.
3. ANSWER 4 OF 6 QUESTIONS ONLY.
4. Staple your question sheet to your answer sheets and turn in.

NRE/MP Radiation Detection & Protection

Answer 4 of the following question.

1. In proton radiotherapy, an attenuator is used to reduce the proton energy. The proton energy from such a machine is 250 MeV. The desired exit energy for the proton is 150 MeV.
   a. How thick must the aluminum attenuator be?
   b. What is the dose rate in tissue due a 150-MeV proton beam with a fluence of 10^{10} protons per cm^2 per second?

PSTAR: Stopping Powers and Range Tables for Protons

MUSCLE, STRIATED (ICRU)

Kinetic Energy MeV	Electron. Stp. Pow. MeV cm2/g	Nuclear Stp. Pow. MeV cm2/g	Total Stp. Pow. MeV cm2/g	CSDA Range g/cm2
1.000E+00	2.583E+02	2.122E-01	2.585E+02	2.465E-03
1.250E+00	2.208E+02	1.734E-01	2.210E+02	3.515E-03
1.500E+00	1.939E+02	1.469E-01	1.940E+02	4.725E-03
1.750E+00	1.734E+02	1.277E-01	1.735E+02	6.090E-03
2.000E+00	1.572E+02	1.130E-01	1.573E+02	7.605E-03
2.250E+00	1.441E+02	1.015E-01	1.442E+02	9.267E-03
2.500E+00	1.332E+02	9.212E-02	1.333E+02	1.107E-02
2.750E+00	1.240E+02	8.439E-02	1.241E+02	1.302E-02
3.000E+00	1.161E+02	7.790E-02	1.162E+02	1.510E-02
3.500E+00	1.033E+02	6.758E-02	1.034E+02	1.967E-02
4.000E+00	9.323E+01	5.973E-02	9.329E+01	2.477E-02
4.500E+00	8.512E+01	5.355E-02	8.517E+01	3.039E-02
5.000E+00	7.842E+01	4.857E-02	7.847E+01	3.651E-02
5.500E+00	7.279E+01	4.445E-02	7.284E+01	4.313E-02
6.000E+00	6.798E+01	4.099E-02	6.802E+01	5.024E-02
6.500E+00	6.382E+01	3.805E-02	6.386E+01	5.783E-02
7.000E+00	6.018E+01	3.550E-02	6.022E+01	6.589E-02
7.500E+00	5.697E+01	3.329E-02	5.700E+01	7.443E-02
8.000E+00	5.412E+01	3.134E-02	5.415E+01	8.343E-02
8.500E+00	5.156E+01	2.961E-02	5.159E+01	9.290E-02
9.000E+00	4.926E+01	2.807E-02	4.928E+01	1.028E-01
9.500E+00	4.717E+01	2.668E-02	4.719E+01	1.132E-01
1.000E+01	4.526E+01	2.543E-02	4.529E+01	1.240E-01
1.250E+01	3.782E+01	2.063E-02	3.784E+01	1.847E-01
1.500E+01	3.263E+01	1.737E-02	3.264E+01	2.560E-01
1.750E+01	2.879E+01	1.502E-02	2.881E+01	3.377E-01
2.000E+01	2.583E+01	1.325E-02	2.585E+01	4.295E-01
2.500E+01	2.155E+01	1.073E-02	2.156E+01	6.423E-01
2.750E+01	1.995E+01	9.802E-03	1.996E+01	7.629E-01
3.000E+01	1.859E+01	9.027E-03	1.860E+01	8.928E-01
3.500E+01	1.642E+01	7.800E-03	1.642E+01	1.179E+00
4.000E+01	1.474E+01	6.872E-03	1.475E+01	1.501E+00
4.500E+01	1.342E+01	6.145E-03	1.342E+01	1.857E+00
5.000E+01	1.234E+01	5.560E-03	1.234E+01	2.246E+00
5.500E+01	1.144E+01	5.079E-03	1.145E+01	2.667E+00
6.000E+01	1.068E+01	4.676E-03	1.069E+01	3.119E+00
6.500E+01	1.003E+01	4.333E-03	1.004E+01	3.602E+00
7.000E+01	9.473E+00	4.039E-03	9.477E+00	4.115E+00
7.500E+01	8.982E+00	3.782E-03	8.986E+00	4.657E+00
8.000E+01	8.548E+00	3.557E-03	8.552E+00	5.228E+00
8.500E+01	8.162E+00	3.358E-03	8.166E+00	5.826E+00
9.000E+01	7.817E+00	3.180E-03	7.820E+00	6.452E+00
9.500E+01	7.506E+00	3.020E-03	7.509E+00	7.105E+00
1.000E+02	7.224E+00	2.877E-03	7.227E+00	7.784E+00
1.250E+02	6.136E+00	2.326E-03	6.139E+00	1.155E+01
1.500E+02	5.396E+00	1.956E-03	5.398E+00	1.591E+01
1.750E+02	4.859E+00	1.689E-03	4.861E+00	2.080E+01
2.000E+02	4.452E+00	1.487E-03	4.453E+00	2.618E+01
2.250E+02	4.133E+00	1.329E-03	4.134E+00	3.202E+01
2.500E+02	3.876E+00	1.202E-03	3.877E+00	3.827E+01

PROTONS IN ALUMINUM

ENERGY	STOPPING POWER			CSDA	DETOUR
	ELECTRONIC	NUCLEAR	TOTAL	RANGE	FACTOR
MeV	MeV cm2/g	MeV cm2/g	MeV cm2/g	g/cm2	
0.001	9.238E+01	1.197E+01	1.043E+02	1.471E-05	0.2555
0.0015	1.131E+02	1.072E+01	1.239E+02	1.906E-05	0.2933
0.002	1.306E+02	9.749E+00	1.404E+02	2.285E-05	0.3245
0.0025	1.461E+02	8.967E+00	1.550E+02	2.623E-05	0.3509
0.003	1.600E+02	8.324E+00	1.683E+02	2.933E-05	0.3738
0.004	1.848E+02	7.322E+00	1.921E+02	3.487E-05	0.4122
0.005	2.066E+02	6.571E+00	2.131E+02	3.981E-05	0.4434
0.006	2.263E+02	5.982E+00	2.323E+02	4.430E-05	0.4696
0.007	2.444E+02	5.505E+00	2.499E+02	4.845E-05	0.4921
0.008	2.613E+02	5.110E+00	2.664E+02	5.232E-05	0.5117
0.009	2.771E+02	4.775E+00	2.819E+02	5.597E-05	0.5291
0.010	2.921E+02	4.488E+00	2.966E+02	5.943E-05	0.5445
0.0125	3.206E+02	3.917E+00	3.245E+02	6.746E-05	0.5773
0.015	3.448E+02	3.491E+00	3.483E+02	7.489E-05	0.6040
0.0175	3.657E+02	3.157E+00	3.689E+02	8.186E-05	0.6263
0.020	3.838E+02	2.889E+00	3.867E+02	8.848E-05	0.6454
0.0225	3.996E+02	2.667E+00	4.022E+02	9.481E-05	0.6620
0.025	4.132E+02	2.480E+00	4.157E+02	1.009E-04	0.6767
0.0275	4.250E+02	2.321E+00	4.273E+02	1.069E-04	0.6898
0.030	4.351E+02	2.183E+00	4.373E+02	1.126E-04	0.7015
0.035	4.510E+02	1.955E+00	4.529E+02	1.239E-04	0.7220
0.040	4.620E+02	1.774E+00	4.638E+02	1.348E-04	0.7394
0.045	4.692E+02	1.627E+00	4.709E+02	1.455E-04	0.7544
0.050	4.734E+02	1.504E+00	4.749E+02	1.560E-04	0.7676
0.055	4.752E+02	1.401E+00	4.766E+02	1.665E-04	0.7793
0.060	4.751E+02	1.311E+00	4.764E+02	1.770E-04	0.7898
0.065	4.737E+02	1.234E+00	4.749E+02	1.875E-04	0.7994
0.070	4.712E+02	1.166E+00	4.724E+02	1.981E-04	0.8081
0.075	4.680E+02	1.106E+00	4.691E+02	2.087E-04	0.8161
0.080	4.642E+02	1.052E+00	4.653E+02	2.194E-04	0.8234
0.085	4.601E+02	1.003E+00	4.611E+02	2.302E-04	0.8302
0.090	4.558E+02	9.597E-01	4.567E+02	2.411E-04	0.8366
0.095	4.513E+02	9.200E-01	4.522E+02	2.521E-04	0.8425
0.100	4.468E+02	8.837E-01	4.477E+02	2.632E-04	0.8480
0.125	4.245E+02	7.406E-01	4.253E+02	3.205E-04	0.8708
0.150	4.045E+02	6.400E-01	4.051E+02	3.808E-04	0.8880
0.175	3.867E+02	5.651E-01	3.873E+02	4.439E-04	0.9013
0.200	3.710E+02	5.070E-01	3.715E+02	5.098E-04	0.9119
0.225	3.568E+02	4.604E-01	3.573E+02	5.785E-04	0.9205
0.250	3.440E+02	4.222E-01	3.444E+02	6.498E-04	0.9277
0.275	3.323E+02	3.903E-01	3.327E+02	7.236E-04	0.9337
0.30	3.215E+02	3.632E-01	3.218E+02	8.001E-04	0.9389
0.35	3.017E+02	3.195E-01	3.020E+02	9.605E-04	0.9471
0.40	2.842E+02	2.858E-01	2.844E+02	1.131E-03	0.9535
0.45	2.686E+02	2.589E-01	2.689E+02	1.312E-03	0.9585
0.50	2.548E+02	2.369E-01	2.550E+02	1.503E-03	0.9626
0.55	2.425E+02	2.185E-01	2.427E+02	1.704E-03	0.9659
0.60	2.314E+02	2.030E-01	2.316E+02	1.915E-03	0.9687
0.65	2.215E+02	1.897E-01	2.216E+02	2.136E-03	0.9711
0.70	2.124E+02	1.781E-01	2.126E+02	2.366E-03	0.9731
0.75	2.042E+02	1.679E-01	2.043E+02	2.606E-03	0.9749
0.80	1.966E+02	1.589E-01	1.968E+02	2.856E-03	0.9764
0.85	1.897E+02	1.509E-01	1.899E+02	3.114E-03	0.9778
0.90	1.833E+02	1.436E-01	1.835E+02	3.382E-03	0.9790
0.95	1.774E+02	1.371E-01	1.775E+02	3.659E-03	0.9800
1.00	1.719E+02	1.312E-01	1.720E+02	3.945E-03	0.9810
1.25	1.494E+02	1.082E-01	1.495E+02	5.509E-03	0.9845
1.50	1.327E+02	9.232E-02	1.328E+02	7.287E-03	0.9868
1.75	1.198E+02	8.066E-02	1.199E+02	9.272E-03	0.9884
2.00	1.094E+02	7.173E-02	1.095E+02	1.146E-02	0.9895
2.25	1.009E+02	6.466E-02	1.010E+02	1.384E-02	0.9904
2.50	9.377E+01	5.891E-02	9.383E+01	1.641E-02	0.9911
2.75	8.769E+01	5.414E-02	8.775E+01	1.916E-02	0.9916
3.0	8.245E+01	5.011E-02	8.250E+01	2.210E-02	0.9921
3.5	7.383E+01	4.369E-02	7.388E+01	2.852E-02	0.9928
4.0	6.703E+01	3.877E-02	6.707E+01	3.563E-02	0.9933

ENERGY	STOPPING POWER			CSDA	DETOUR
	ELECTRONIC	NUCLEAR	TOTAL	RANGE	FACTOR
MeV	MeV cm2/g	MeV cm2/g	MeV cm2/g	g/cm2	
4.5	6.151E+01	3.489E-02	6.154E+01	4.343E-02	0.9937
5.0	5.691E+01	3.174E-02	5.695E+01	5.188E-02	0.9940
5.5	5.303E+01	2.913E-02	5.306E+01	6.098E-02	0.9942
6.0	4.970E+01	2.693E-02	4.973E+01	7.072E-02	0.9944
6.5	4.681E+01	2.505E-02	4.684E+01	8.109E-02	0.9946
7.0	4.428E+01	2.342E-02	4.430E+01	9.207E-02	0.9948
7.5	4.203E+01	2.200E-02	4.205E+01	1.037E-01	0.9949
8.0	4.002E+01	2.075E-02	4.004E+01	1.158E-01	0.9950
8.5	3.822E+01	1.963E-02	3.824E+01	1.286E-01	0.9951
9.0	3.658E+01	1.864E-02	3.660E+01	1.420E-01	0.9952
9.5	3.510E+01	1.774E-02	3.512E+01	1.559E-01	0.9953
10.0	3.375E+01	1.693E-02	3.376E+01	1.705E-01	0.9953
12.5	2.841E+01	1.380E-02	2.842E+01	2.515E-01	0.9956
15.0	2.465E+01	1.166E-02	2.466E+01	3.462E-01	0.9958
17.5	2.185E+01	1.012E-02	2.186E+01	4.541E-01	0.9960
20.0	1.968E+01	8.940E-03	1.969E+01	5.748E-01	0.9961
22.5	1.794E+01	8.014E-03	1.795E+01	7.080E-01	0.9962
25.0	1.651E+01	7.266E-03	1.652E+01	8.533E-01	0.9963
27.5	1.532E+01	6.649E-03	1.532E+01	1.011E+00	0.9963
30.0	1.430E+01	6.130E-03	1.431E+01	1.180E+00	0.9964
35.0	1.267E+01	5.308E-03	1.268E+01	1.552E+00	0.9965
40.0	1.141E+01	4.684E-03	1.142E+01	1.968E+00	0.9966
45.0	1.041E+01	4.194E-03	1.041E+01	2.427E+00	0.9966
50.0	9.590E+00	3.798E-03	9.594E+00	2.928E+00	0.9967
55.0	8.908E+00	3.473E-03	8.911E+00	3.469E+00	0.9968
60.0	8.330E+00	3.200E-03	8.334E+00	4.050E+00	0.9968
65.0	7.835E+00	2.967E-03	7.838E+00	4.669E+00	0.9968
70.0	7.405E+00	2.767E-03	7.408E+00	5.325E+00	0.9969
75.0	7.029E+00	2.593E-03	7.031E+00	6.018E+00	0.9969
80.0	6.696E+00	2.439E-03	6.698E+00	6.747E+00	0.9970
85.0	6.399E+00	2.304E-03	6.401E+00	7.511E+00	0.9970
90.0	6.133E+00	2.182E-03	6.135E+00	8.309E+00	0.9970
95.0	5.893E+00	2.074E-03	5.895E+00	9.141E+00	0.9970
100.0	5.676E+00	1.976E-03	5.678E+00	1.001E+01	0.9971
125.0	4.835E+00	1.600E-03	4.837E+00	1.480E+01	0.9972
150.0	4.261E+00	1.346E-03	4.262E+00	2.032E+01	0.9973
175.0	3.843E+00	1.163E-03	3.844E+00	2.651E+01	0.9973
200.0	3.525E+00	1.025E-03	3.526E+00	3.331E+01	0.9974
225.0	3.276E+00	9.164E-04	3.277E+00	4.067E+01	0.9975
250.0	3.075E+00	8.293E-04	3.076E+00	4.855E+01	0.9975
275.0	2.910E+00	7.576E-04	2.911E+00	5.691E+01	0.9976
300.0	2.772E+00	6.976E-04	2.773E+00	6.572E+01	0.9976
350.0	2.555E+00	6.027E-04	2.555E+00	8.454E+01	0.9977
400.0	2.392E+00	5.311E-04	2.393E+00	1.048E+02	0.9978
450.0	2.266E+00	4.750E-04	2.267E+00	1.263E+02	0.9979
500.0	2.166E+00	4.299E-04	2.167E+00	1.489E+02	0.9979
550.0	2.086E+00	3.928E-04	2.086E+00	1.724E+02	0.9980
600.0	2.019E+00	3.617E-04	2.020E+00	1.968E+02	0.9980
650.0	1.964E+00	3.353E-04	1.965E+00	2.219E+02	0.9981
700.0	1.918E+00	3.126E-04	1.918E+00	2.476E+02	0.9981
750.0	1.878E+00	2.929E-04	1.879E+00	2.740E+02	0.9982
800.0	1.845E+00	2.755E-04	1.845E+00	3.008E+02	0.9982
850.0	1.816E+00	2.602E-04	1.816E+00	3.282E+02	0.9982
900.0	1.790E+00	2.465E-04	1.791E+00	3.559E+02	0.9983
950.0	1.768E+00	2.342E-04	1.769E+00	3.840E+02	0.9983
1000.0	1.749E+00	2.232E-04	1.750E+00	4.124E+02	0.9983
1500.0	1.647E+00	1.523E-04	1.647E+00	7.087E+02	0.9986
2000.0	1.617E+00	1.161E-04	1.618E+00	1.016E+03	0.9987
2500.0	1.613E+00	9.419E-05	1.613E+00	1.325E+03	0.9989
3000.0	1.619E+00	7.938E-05	1.619E+00	1.635E+03	0.9990
4000.0	1.642E+00	6.062E-05	1.642E+00	2.248E+03	0.9991
5000.0	1.668E+00	4.920E-05	1.668E+00	2.853E+03	0.9992
6000.0	1.692E+00	4.148E-05	1.692E+00	3.448E+03	0.9993
7000.0	1.714E+00	3.592E-05	1.714E+00	4.035E+03	0.9993
8000.0	1.734E+00	3.170E-05	1.734E+00	4.615E+03	0.9994
9000.0	1.752E+00	2.840E-05	1.752E+00	5.189E+03	0.9994
10000.0	1.768E+00	2.574E-05	1.768E+00	5.757E+03	0.9995

2. Sr-82 is made at the LANSCE accelerator at LANL using Rb as a target material. It is formed by the $^{85}Rb(p,4n)^{82}Sr$ reaction. The decay product of ^{82}Sr, ^{82}Rb, is used in PET scanning applications

   a. What is the Q-value of the reaction?

   b. Targets of RbCl are placed in a proton beam to produce the ^{82}Sr. The target assembly has several target layers and, according to the Number 30, 2006 issue of *Los Alamos Science*, the Rb target is placed at a location at which the proton energy has degraded to between 45 and 65 MeV. The protons are initially at 100 MeV. According to a 2002 talk on radioisotope production at LANL, the yield of Sr-82 yield ranges from 0.05 mCi/microamp-hr for protons at 45 MeV to 0.29 mCi/microamp-hr for protons at 65 MeV. Assume that the production rate is 0.2 mCi/microamp-hr. If the target is placed in an 80 microamp beam current and contains 8 grams of RbCl, how long must it be irradiated to obtain 700 mCi of ^{82}Sr.

   c. If all the ^{82}Sr is immediately extracted, what is the photon dose rate in tissue at 1 meter from the specimen <u>five minutes</u> after it is removed? Ignore air attenuation.

Isotope	Decay mode	Energy of Photon Emitted	Probability per decay
^{82}Sr	Electron capture	----	----
^{82}Rb	Positron emission (96%) electron capture (4%)	0.777	9%

<u>Elemental Atomic Masses</u>:

Rb 85.4678 amu
Sr 87.62 amu
Cl 35.453 amu

Nuclear Wallet Cards

Nuclide Z El	A	Jπ	Δ (MeV)	T½, Γ, or Abundance	Decay Mode
38 Sr	81	1/2–	–71.528	22.3 m 4	ε
	82	0+	–76.008	25.55 d 15	ε
	83	7/2+	–76.80	32.41 h 3	ε
	83m	1/2–	–76.54	4.95 s 12	IT
	84	0+	–80.644	**0.56% 1**	
	85	9/2+	–81.103	64.84 d 2	ε
	85m	1/2–	–80.864	67.63 m 4	IT 86.6%, ε 13.4%
	86	0+	–84.524	**9.86% 1**	
	87	9/2+	–84.880	**7.00% 1**	
	87m	1/2–	–84.492	2.815 h 12	IT 99.7%, ε 0.3%
	88	0+	–87.922	**82.58% 1**	
	89	5/2+	–86.209	50.57 d 3	β–
	90	0+	–85.942	28.90 y 3	β–
	91	5/2+	–83.645	9.63 h 5	β–
	92	0+	–82.868	2.66 h 4	β–
	93	5/2+	–80.085	7.423 m 24	β–
	94	0+	–78.840	75.3 s 2	β–
	95	1/2+	–75.117	23.90 s 14	β–
	96	0+	–72.94	1.07 s 1	β–
	97	1/2+	–68.79	429 ms 5	β–, β–n≤0.05%
	98	0+	–66.65	0.653 s 2	β–, β–n 0.25%
	99	3/2+	–62.19	0.269 s 1	β–, β–n 0.1%
	100	0+	–60.2	202 ms 3	β–, β–n 0.78%
	101	(5/2–)	–55.4	118 ms 3	β–, β–n 2.37%
	102	0+	–53.1	69 ms 6	β–, β–n 4.8%
	103		–47.6s	>150 ns	β–
	104	0+	–44.4s	>300 ns	
	105		–38.6s	>150 ns	β–
39 Y	76		–38.7s	>200 ns	ε?, p?
	77		–46.90s	≈0.06 s	ε, εp
	78	(0+)	–52.5s	50 ms 8	ε
	78m	(5+)	–52.5s	5.7 s 7	ε
	79	(5/2+)	–58.4	14.8 s 6	ε, εp
	80	(4–)	–61.2	30.1 s 5	ε, εp
	80m	(1–)	–61.0	4.8 s 3	IT 81%, ε 19%
	81	(5/2+)	–66.02	70.4 s 10	ε
	82	1+	–68.2	8.30 s 20	ε
	83	9/2+	–72.33	7.08 m 6	ε
	83m	3/2–	–72.26	2.85 m 2	ε 60%, IT 40%
	84	1+	–74.16	4.6 s 2	ε
	84m	(5–)	–74.16	39.5 m 8	ε
	85	(1/2)–	–77.84	2.68 h 5	ε
	85m	9/2+	–77.82	4.86 h 13	ε, IT<2.0×10^{-3}%
	86	4–	–79.28	14.74 h 2	ε
	86m	(8+)	–79.07	48 m 1	IT 99.31%, ε 0.69%
	87	1/2–	–83.019	79.8 h 3	ε
	87m	9/2+	–82.638	13.37 h 3	IT 98.43%, ε 1.57%
	88	4–	–84.299	106.616 d 13	ε
	89	1/2–	–87.702	**100%**	
	89m	9/2+	–86.793	15.28 s 17	IT
	90	2–	–86.488	64.053 h 20	β–
	90m	7+	–85.806	3.19 h 6	IT, β– 1.8×10^{-3}%

Nuclear Wallet Cards

Nuclide Z El	A	Jπ	Δ (MeV)	T½, Γ, or Abundance	Decay Mode
39 Y	91	1/2–	–86.345	58.51 d 6	β–
	91m	9/2+	–85.789	49.71 m 4	IT, β–<1.5%
	92	2–	–84.813	3.54 h 1	β–
	93	1/2–	–84.22	10.18 h 8	β–
	93m	7/2+	–83.46	0.82 s 4	IT
	94	2–	–82.349	18.7 m 1	β–
	95	1/2–	–81.207	10.3 m 1	β–
	96	0–	–78.35	5.34 s 5	β–
	96m	(8)+	–78.35	9.6 s 2	β–
	97	(1/2–)	–76.26	3.75 s 3	β–, β–n 0.058%
	97m	(9/2)+	–75.59	1.17 s 3	β–>99.3%, IT<0.7%, β–n<0.08%
	97m	(27/2–)	–72.73	142 ms 8	IT>80%, β–<20%
	98	(0)–	–72.47	0.548 s 2	β–, β–n 0.33%
	98m	(4,5)	–72.06	2.0 s 2	β–>80%, IT<20%, β–n 3.4%
	99	(5/2+)	–70.20	1.470 s 7	β–, β–n 1.9%
	100	1–,2–	–67.29	735 ms 7	β–, β–n 0.92%
	100m	(3,4,5)	–67.29	0.94 s 3	β–
	101	(5/2+)	–64.91	0.45 s 2	β–, β–n 1.5%
	102m		–61.89	0.30 s 1	β–, β–n 4%
	102m		–61.89	0.36 s 4	β–, β–n 4%
	103	(5/2+)	–58.9s	0.23 s 2	β–, β–n 8%
	104		–54.9s	180 ms 60	β–, β–n?
	105		–51.4s	>300 ns	β–?
	106		–46.8s	>150 ns	β–
	107	(5/2+)	–42.7s	≈30 ms	β–
	108		–37.7s	20 ms *sy*	β–, β–n
40 Zr	78	0+	–41.7s	>200 ns	ε?, εp?
	79		–47.4s	56 ms 30	ε, εp
	80	0+	–56	4.6 s 6	ε, εp
	81	(3/2–)	–58.5	5.5 s 4	ε, εp 0.12%
	82	0+	–64.2s	32 s 5	ε
	83	(1/2–)	–66.46	41.6 s 24	ε, εp
	84	0+	–71.5s	25.9 m 7	ε
	85	7/2+	–73.1	7.86 m 4	ε
	85m	(1/2–)	–72.9	10.9 s 3	IT≤92%, ε>8%
	86	0+	–77.80	16.5 h 1	ε
	87	(9/2)+	–79.348	1.68 h 1	ε
	87m	(1/2)–	–79.012	14.0 s 2	IT
	88	0+	–83.62	83.4 d 3	ε
	89	9/2+	–84.869	78.41 h 12	ε
	89m	1/2–	–84.281	4.161 m 17	IT 93.77%, ε 6.23%
	90	0+	–88.767	**51.45% 40**	
	90m	5–	–86.448	809.2 ms 20	IT
	91	5/2+	–87.890	**11.22% 5**	
	92	0+	–88.454	**17.15% 8**	
	93	5/2+	–87.117	1.53×10^{6} y 10	β–
	94	0+	–87.267	**17.38% 28**	
	95	5/2+	–85.658	64.032 d 6	β–
	96	0+	–85.443	>3.9×10^{20} y **2.80% 9**	2β–

Nuclear Wallet Cards

Nuclide Z El	A	Jπ	Δ (MeV)	T½, Γ, or Abundance	Decay Mode
35 Br	82	5−	−77.496	35.282 h 7	β−
	82m	2−	−77.451	6.13 m 5	IT 97.6%, β− 2.4%
	83	3/2−	−79.009	2.40 h 2	β−
	84	2−	−77.80	31.80 m 8	β−
	84m	6−	−77.48	6.0 m 2	β−
	85	3/2−	−78.61	2.90 m 6	β−
	86	(2−)	−75.64	55.1 s 4	β−
	87	3/2−	−73.86	55.65 s 13	β−, β−n 2.6%
	88	(2−)	−70.73	16.29 s 6	β−, β−n 6.58%
	89	(3/2−,5/2−)	−68.57	4.40 s 3	β−, β−n 13.8%
	90		−64.62	1.91 s 1	β−, β−n 25.2%
	91		−61.51	0.541 s 5	β−, β−n 20%
	92	(2−)	−56.58	0.343 s 15	β−, β−n 33.1%
	93	(5/2−)	−53.0s	102 ms 10	β−, β−n 68%
	94		−47.8s	70 ms 20	β−, β−n 70%
	95	(3/2−)	−43.9s	>150 ns	β−
	96		−38.6s	>150 ns	β−
	97	(3/2−)	−34.7s	>150 ns	β−
36 Kr	69		−32.4s	32 ms 10	ε
	70	0+	−41.7s	52 ms 17	ε, εp≤1.3%
	71	(5/2)−	−46.9	100 ms 3	ε, εp 5.2%
	72	0+	−53.941	17.1 s 2	ε
	73	3/2−	−56.552	27.3 s 10	ε, εp 0.25%
	74	0+	−62.332	11.50 m 11	ε
	75	5/2+	−64.324	4.29 m 17	ε
	76	0+	−69.014	14.8 h 1	ε
	77	5/2+	−70.169	74.4 m 6	ε
	78	0+	−74.180	≥2.3×10^{20} y **0.35% 1**	2ε
	79	1/2−	−74.443	35.04 h 10	ε
	79m	7/2+	−74.313	50 s 3	IT
	80	0+	−77.893	**2.28% 6**	
	81	7/2+	−77.694	2.29×10^{5} y 11	ε
	81m	1/2−	−77.503	13.10 s 3	IT, ε 2.5×10^{-3}%
	82	0+	−80.590	**11.58% 14**	
	83	9/2+	−79.982	**11.49% 6**	
	83m	1/2−	−79.940	1.83 h 2	IT
	84	0+	−82.431	**57.00% 4**	
	85	9/2+	−81.480	3916.8 d 25	β−
	85m	1/2−	−81.175	4.480 h 8	β− 78.6%, IT 21.4%
	86	0+	−83.266	**17.30% 22**	
	87	5/2+	−80.709	76.3 m 5	β−
	88	0+	−79.69	2.84 h 3	β−
	89	3/2(+)	−76.73	3.15 m 4	β−
	90	0+	−74.97	32.32 s 9	β−
	91	5/2(+)	−71.31	8.57 s 4	β−
	92	0+	−68.79	1.840 s 8	β−, β−n 0.03%
	93	1/2+	−64.0	1.286 s 10	β−, β−n 1.95%
	94	0+	−61.1s	212 ms 5	β−, β−n 1.26%
	95	1/2	−56.0s	114 ms 3	β−, β−n 2.87%
	96	0+	−53.0s	80 ms 8	β−, β−n 3.8%
	97		−47.9s	63 ms 4	β−, β−n 8.2%

Nuclear Wallet Cards

Nuclide Z El	A	Jπ	Δ (MeV)	T½, Γ, or Abundance	Decay Mode
36 Kr	98	0+	−44.8s	46 ms 8	β−, β−n 7%
	99	(3/2+)	−39.5s	40 ms 11	β−, β−n 11%
	100	0+	−36.2s	>150 ns	β−
37 Rb	71		−32.3s	?	p?
	72	(3+)	−38.1s	<1.2 μs	p
	73		−46.1s	>30 ns	ε, p>0%
	74	(0+)	−51.917	64.9 ms 5	ε
	75	(3/2−)	−57.222	19.0 s 12	ε
	76	1(−)	−60.480	36.5 s 6	ε, εα 3.8×10^{-7}%
	77	3/2−	−64.825	3.77 m 4	ε
	78	0(+)	−66.936	17.66 m 8	ε
	78m	4(−)	−66.833	5.74 m 5	ε 90%, IT 10%
	79	5/2+	−70.803	22.9 m 5	ε
	80	1+	−72.173	33.4 s 7	ε
	81	3/2−	−75.455	4.570 h 4	ε
	81m	9/2+	−75.368	30.5 m 3	IT 97.6%, ε 2.4%
	82	1+	−76.188	1.273 m 2	ε
	82m	5−	−76.119	6.472 h 5	ε, IT<0.33%
	83	5/2−	−79.075	86.2 d 1	ε
	84	2−	−79.750	33.1 d 1	ε 96.2%, β− 3.8%
	84m	6−	−79.286	20.26 m 4	IT
	85	5/2−	−82.167	**72.17% 2**	
	86	2−	−82.747	18.642 d 18	β− 99.99%, ε 5.2×10^{-3}%
	86m	6−	−82.191	1.017 m 3	IT, β−<0.3%
	87	3/2−	−84.598	4.97×10^{10} y 3 **27.83% 2**	β−
	88	2−	−82.609	17.773 m 11	β−
	89	3/2−	−81.713	15.15 m 12	β−
	90	0−	−79.362	158 s 5	β−
	90m	3−	−79.255	258 s 4	β− 97.4%, IT 2.6%
	91	3/2(−)	−77.745	58.4 s 4	β−
	92	0−	−74.772	4.492 s 20	β−, β−n 0.01%
	93	5/2−	−72.618	5.84 s 2	β−, β−n 1.39%
	94	3(−)	−68.553	2.702 s 5	β−, β−n 10.01%
	95	5/2−	−65.85	377.5 ms 8	β−, β−n 8.73%
	96	2+	−61.22	202.8 ms 33	β−, β−n 14%
	97	3/2+	−58.36	169.9 ms 7	β−, β−n 25.1%
	98	(0,1)	−54.22	114 ms 5	β−, β−n 13.8%, β− 0.05%
	99	(5/2+)	−50.9	50.3 ms 7	β−, β−n 15.9%
	100		−46.7s	51 ms 8	β−, β−n 6%, β−2n 0.16%
	101	(3/2+)	−43.6	32 ms 5	β−, β−n 28%
38 Sr	73		−31.7s	>25 ms	ε, εp>0%
	74	0+	−40.7s	>1.2 μs	ε
	75	(3/2−)	−46.6	88 ms 3	ε, εp 5.2%
	76	0+	−54.24	7.89 s 7	ε, εp 0.34%
	77	5/2+	−57.804	9.0 s 2	ε, εp<0.25%
	78	0+	−63.174	2.5 m 3	ε
	79	3/2(−)	−65.477	2.25 m 10	ε
	80	0+	−70.308	106.3 m 15	ε

19

Table C.7 *(cont.)* Mass interaction (total-coherent), energy transfer, and energy absorption coefficients (cm^2/g) for various compounds and mixtures.

E (MeV)	ICRU-tissue[a]			LiF[b]			NaI[c]		
	μ/ρ	μ_{tr}/ρ	μ_{en}/ρ	μ/ρ	μ_{tr}/ρ	μ_{en}/ρ	μ/ρ	μ_{tr}/ρ	μ_{en}/ρ
0.01	4.716	4.565	4.564	5.857	5.735	5.733	1.376+2	1.334+2	1.334+2
0.015	1.430	1.267	1.266	1.746	1.613	1.612	4.579+1	4.479+1	4.475+1
0.02	6.763−1	5.072−1	5.070−1	7.887−1	6.497−1	6.494−1	2.071+1	2.031+1	2.028+1
0.03	3.153−1	1.439−1	1.438−1	3.248−1	1.827−1	1.826−1	6.714+0	6.547+0	6.531+0
0.03317							5.081+0	4.933+0	4.920+0
0.03317 K							2.986+1	1.013+1	1.012+1
0.04	2.333−1	6.476−2	6.474−2	2.193−1	7.895−2	7.890−2	1.835+1	8.185+0	8.174+0
0.05	2.037−1	3.988−2	3.987−2	1.823−1	4.543−2	4.541−2	1.017+1	5.594+0	5.583+0
0.06	1.891−1	3.053−2	3.051−2	1.649−1	3.225−2	3.223−2	6.229+0	3.847+0	3.837+0
0.08	1.734−1	2.531−2	2.530−2	1.480−1	2.386−2	2.385−2	2.863+0	1.989+0	1.981+0
0.10	1.636−1	2.502−2	2.501−2	1.386−1	2.230−2	2.229−2	1.576+0	1.149+0	1.142+0
0.15	1.466−1	2.733−2	2.732−2	1.235−1	2.333−2	2.332−2	5.663−1	4.099−1	4.060−1
0.20	1.343−1	2.938−2	2.936−2	1.131−1	2.485−2	2.484−2	3.019−1	2.011−1	1.988−1
0.30	1.169−1	3.164−2	3.161−2	9.835−2	2.666−2	2.663−2	1.534−1	8.403−2	8.280−2
0.40	1.048−1	3.250−2	3.247−2	8.817−2	2.737−2	2.734−2	1.100−1	5.316−2	5.228−2
0.50	9.572−2	3.272−2	3.267−2	8.053−2	2.753−2	2.749−2	9.035−2	4.132−2	4.056−2
0.60	8.855−2	3.257−2	3.252−2	7.451−2	2.741−2	2.736−2	7.900−2	3.557−2	3.485−2
0.80	7.781−2	3.182−2	3.175−2	6.548−2	2.678−2	2.671−2	6.571−2	3.007−2	2.935−2
1.00	6.998−2	3.081−2	3.073−2	5.888−2	2.592−2	2.585−2	5.762−2	2.728−2	2.652−2
1.25	6.259−2	2.946−2	2.937−2	5.267−2	2.479−2	2.470−2	5.087−2	2.508−2	2.424−2
1.50	5.696−2	2.817−2	2.806−2	4.795−2	2.371−2	2.361−2	4.644−2	2.365−2	2.275−2
2.00	4.892−2	2.596−2	2.582−2	4.120−2	2.186−2	2.173−2	4.119−2	2.222−2	2.117−2
3.00	3.928−2	2.277−2	2.258−2	3.320−2	1.926−2	1.907−2	3.668−2	2.193−2	2.053−2
4.00	3.367−2	2.069−2	2.044−2	2.856−2	1.758−2	1.733−2	3.512−2	2.283−2	2.100−2
5.00	2.998−2	1.924−2	1.894−2	2.554−2	1.644−2	1.614−2	3.472−2	2.410−2	2.179−2
6.00	2.739−2	1.821−2	1.785−2	2.343−2	1.564−2	1.528−2	3.484−2	2.543−2	2.263−2
8.00	2.400−2	1.685−2	1.638−2	2.069−2	1.462−2	1.414−2	3.583−2	2.811−2	2.423−2
10.00	2.191−2	1.604−2	1.546−2	1.903−2	1.403−2	1.345−2	3.722−2	3.061−2	2.560−2
15.00	1.913−2	1.505−2	1.420−2	1.687−2	1.338−2	1.253−2	4.081−2	3.588−2	2.794−2
20.00	1.785−2	1.470−2	1.360−2	1.592−2	1.323−2	1.211−2	4.385−2	3.988−2	2.908−2
30.00	1.681−2	1.463−2	1.305−2	1.523−2	1.336−2	1.174−2	4.869−2	4.579−2	2.969−2
40.00	1.648−2	1.481−2	1.276−2	1.508−2	1.365−2	1.154−2	5.221−2	4.991−2	2.921−2
50.00	1.642−2	1.507−2	1.256−2	1.513−2	1.396−2	1.138−2	5.498−2	5.306−2	2.839−2
60.00	1.646−2	1.532−2	1.239−2	1.524−2	1.425−2	1.123−2	5.720−2	5.555−2	2.745−2
80.00	1.667−2	1.580−2	1.206−2	1.552−2	1.477−2	1.092−2	6.052−2	5.924−2	2.554−2
100.0	1.692−2	1.621−2	1.173−2	1.580−2	1.519−2	1.060−2	6.297−2	6.191−2	2.384−2

[a] ICRU-33 four-component approximation. Composition by weight fraction: H 0.101174, C 0.111000, N 0.026000, O 0.761826. Density 1.00 g cm^{-3}.

[b] Density 2.635 g cm^{-3}. Composition by weight fraction: Li 0.267585 F 0.732415.

[c] Density 3.67 g cm^{-3}. Composition by weight fraction: Na 0.153374 I 0.846626.

3. At the end of last year, Po-210 was used to murder a former spy. Po-210 decays by alpha emission to Pb-206 (stable).
   a. What is the kinetic energy of the emitted alpha particle?
   b. Po-210 is distributed uniformly throughout the body. If an 80 kg man has 40 MBq of Po-210 distributed throughout his body, what is his absorbed dose rate in Gy?
   c. What amount of activity of Sr-90 in secular equilibrium with its progeny Y-90 would lead to the same absorbed dose rate? Both are pure beta emitters. Ignore the dose rate due to bremsstrahlung. The maximum beta energies for Sr-90 and Y-90 are 0.546 and 2.284 MeV, respectively.

Results for Z=82

Nucleus	E(level) (MeV)	Jπ	Δ(MeV)	$T_{1/2}$	Abundance	Decay Modes
$^{200}_{82}$Pb	0.0000	0+	-26.2433	21.5 h *4*		• : 100.00 %
$^{201}_{82}$Pb	0.0000	5/2-	-25.2570	9.33 h *3*		• : 100.00 %
$^{201m}_{82}$Pb	0.6291	13/2+	-24.6279	60.8 s *18*		IT • 100.00 %
$^{202}_{82}$Pb	0.0000	0+	-25.9336	52.5E+3 y *28*		• : 100.00 % • < 1.00 %
$^{202m}_{82}$Pb	2.1698	9-	-23.7638	3.53 h *1*		IT : 90.50 % • : 9.50 %
$^{203}_{82}$Pb	0.0000	5/2-	-24.7866	51.92 h *3*		• : 100.00 %
$^{203m}_{82}$Pb	0.8252	13/2+	-23.9614	6.21 s *11*		IT : 100.00 %
$^{203m}_{82}$Pb	2.9492	29/2-	-21.8374	480 ms *7*		IT : 100.00 %
$^{204}_{82}$Pb	0.0000	0+	-25.1097	• 1.4E+17 y	1.4% *1*	• ?
$^{204m}_{82}$Pb	2.1858	9-	-22.9239	67.2 m *3*		IT : 100.00 %
$^{205}_{82}$Pb	0.0000	5/2-	-23.7701	1.73E+7 y *7*		• : 100.00 %
$^{205m}_{82}$Pb	1.0138	13/2+	-22.7562	5.55 ms *2*		IT : 100.00 %
$^{206}_{82}$Pb	0.0000	0+	-23.7850	STABLE	24.1% *1*	
$^{206m}_{82}$Pb	2.2001	7-	-21.5849	125 µS *2*		IT : 100.00 %
$^{206m}_{82}$Pb	4.0273	12+	-19.7577	202 ns *3*		IT : 100.00 %
$^{207}_{82}$Pb	0.0000	1/2-	-22.4519	STABLE	22.1% *1*	
$^{207m}_{82}$Pb	1.6334	13/2+	-20.8185	0.806 s *6*		IT : 100.00 %
$^{208}_{82}$Pb	0.0000	0+	-21.7485	STABLE	52.4% *1*	
$^{209}_{82}$Pb	0.0000	9/2+	-17.6144	3.253 h *14*		•$^-$: 100.00 %
$^{210}_{82}$Pb	0.0000	0+	-14.7283	22.20 y *22*		•$^-$: 100.00 % • : 1.9E-6 %

Nuclear Wallet Cards

Nuclide Z El A	Jπ	Δ (MeV)	T½, Γ, or Abundance	Decay Mode
84 Po 191	(3/2−)	−5.05	22 ms *1*	α
191m	(13/2+)	−4.92	93 ms *3*	α
192	0+	−8.07	33.2 ms *14*	α≈99.5%, ε≈0.5%
193m	(13/2+)	−8.36	243 ms +*11*−*10*	α≤100%
193m	(3/2−)	−8.36	370 ms +*46*−*40*	α≤100%
194	0+	−11.01	0.392 s *4*	α≈100%, ε
195	(3/2−)	−11.07	4.64 s *9*	α 75%, ε 25%
195m	(13/2+)	−10.84	1.92 s *2*	α≈90%, ε≈10%, IT<0.01%
196	0+	−13.47	5.8 s *2*	α≈98%, ε≈2%
197	(3/2−)	−13.36	84 s *16*	ε 56%, α 44%
197m	(13/2+)	−13.15	32 s *2*	α 84%, ε 16%, IT 0.01%
198	0+	−15.47	1.77 m *3*	α 57%, ε 43%
199	(3/2−)	−15.22	4.58 m *52*	ε 92.5%, α 7.5%
199m	13/2+	−14.90	4.13 m *43*	ε 73.5%, α 24%, IT 2.5%
200	0+	−16.95	10.9 m *11*	ε 88.9%, α 11.1%
201	3/2−	−16.525	15.3 m *2*	ε 98.4%, α 1.6%
201m	13/2+	−16.101	8.9 m *2*	IT 56%, ε 41%, α≈2.9%
202	0+	−17.92	44.7 m *5*	ε 98.08%, α 1.92%
203	5/2−	−17.31	36.7 m *5*	ε 99.89%, α 0.11%
203m	13/2+	−16.67	45 s *2*	IT
204	0+	−18.33	3.53 h *2*	ε 99.34%, α 0.66%
205	5/2−	−17.51	1.74 h *8*	ε 99.96%, α 0.04%
206	0+	−18.182	8.8 d *1*	ε 94.55%, α 5.45%
207	5/2−	−17.146	5.80 h *2*	ε 99.98%, α 0.02%
207m	19/2−	−15.763	2.79 s *8*	IT
208	0+	−17.469	2.898 y *2*	α, ε
209	1/2−	−16.366	102 y *5*	α 99.52%, ε 0.48%
210	0+	−15.953	138.376 d *2*	α
211	9/2+	−12.432	0.516 s *3*	α
211m	(25/2+)	−10.970	25.2 s *6*	α 99.98%, IT 0.02%
212m	(18+)	−7.447	45.1 s *6*	α 99.93%
213	9/2+	−6.653	3.65 μs *4*	α
214	0+	−4.470	164.3 μs *20*	α
215	9/2+	−0.540	1.781 ms *4*	α, β− 2.3×10^{-4}%
216	0+	1.784	0.145 s *2*	α
217	(9/2+)	5.901	1.53 s *5*	α
218	0+	8.358	3.10 m *2*	α 99.98%, β− 0.02%
219		12.8s	≈2 m	α?, β−?
220	0+	15.5s	>300 ns	β−?
85 At 191	(1/2+)		1.7 ms +*11*−*5*	α
191m	(7/2−)		2.1 ms +*4*−*3*	α
193	(1/2+)	−0.15	28 ms +*5*−*4*	α≈100%
193m	(7/2−)	−0.14	21 ms *5*	α≈100%
193m	(13/2+)	−0.11	27 ms +*4*−*5*	α 24%
194m		−1.2	≈40 ms	α, ε
194m		−1.2	≈250 ms	α, ε, IT
195	(1/2+)	−3.476	328 ms +*20*	α
195m	(7/2−)	−3.439	147 ms +*5*	α

4. Describe the three sets of neutron detectors used to cover the entire power range (including source start-up range, intermediate range, and power range) of a pressured water reactor (PWR), and explain why a particular set of the detectors is used for each power range.

5. In a positron emission tomography (PET) camera, a ring of BGO detectors are used to detect the coincident events of positron annihilations. Use the following data and the Attachment A to: (a) estimate the energy resolution of the photopeak for the 511-keV photons, and (b) estimate the camera's efficiency for detecting the coincident events.

   Data: thickness of BGO = 2 cm, light collection efficiency = 0.8, and quantum efficiency of photocathode = 0.25.

6. To analyze a urine sample for suspected contamination with alpha-emitting actinides, 20 ml of the urine sample was fully evaporated and the solid content was precipitated and deposited uniformly onto a planchet disk of 2 cm in diameter. The net weight of the solid content on the planchet disk was determined to be 1 mg. The sample disk was then placed in front of a thin-window gas-flow proportional counter to measure alpha events. The alpha background was determined to be 0.05 $\pm$ 0.001 cpm.

   a. If one recorded 8 alpha events in 1 hour, what is the total activity (in Bq) of the alpha-emitting actinides in the sample? (Be sure that you include uncertainty in the answer)
   b. If one tries to count the sample for another hour, what is the probability that he or she will record fewer than 5 counts in that hour?

Right click to open our web site in your browser:
www.detectors.saint-gobain.com

BGO
Bismuth Germanate Scintillation Material

Bismuth Germanate (BGO) is a high Z, high density scintillation material with chemical composition $Bi_4Ge_3O_{12}$. Due to the high atomic number of bismuth (83) and its high density, BGO is a very efficient γ-ray absorber.

BGO is a relatively hard, rugged, non-hygroscopic crystal which does not cleave. The material does not show any significant self-absorption of the scintillation light. BGO can be machined to various shapes and geometries. The crystal housing can be simple since no hermetic sealing is required.

The scintillation emission maximum of BGO is situated at 480nm. Figure 1 shows the emission spectrum. The light emission in photons/keV is about 15-20% of NaI(Tl); but, since the emission is partly in the area above 500nm where phototubes are less sensitive, the relative photoelectron yield of a bialkali PMT compared to NaI(Tl) amounts to 10-15%.

Figure 2 shows a pulse height spectrum obtained by irradiating a BGO crystal with 662 keV γ-rays.

Due to the high Z value of the material, the photofraction for γ-ray absorption is high; and BGO scintillation crystals are used in applications where a high photofraction is required (for example, PET scanners) or because of its high detection efficiency (for example, Compton suppression spectrometers). It is a combination of properties that make BGO the material of choice for neutron activation analysis. Figure 4 shows the photopeak efficiency (also called the photofraction) – the ratio of the number of counts in the total absorption photopeak to the total number of counts as a function of the γ-ray energy for 38mm diameter, 38mm high (1.5" x 1.5") NaI(Tl) and BGO crystals.

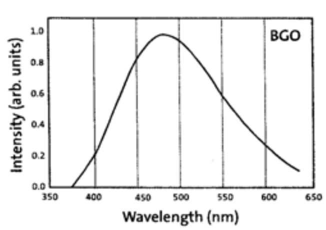

Figure 1. Scintillation emission spectrum of BGO

Properties –

Density [g/cm³]	7.13
Melting point [K]	1323
Thermal expansion coefficient [C⁻¹]	7 x 10⁻⁶
Cleavage plane	none
Hardness (Mho)	5
Hygroscopic	no
Wavelength of emission max. [nm]	480
Lower wavelength cutoff [nm]	320
Refractive index @ emission max	2.15
Primary decay time [ns]	300
Light yield [photons/keVγ]	8-10
Photoelectron yield [% of NaI(Tl)] (for γ-rays)	15 - 20
Temperature response	-1.2%/C
Neutron capture cross-section	1.47b
Afterglow@20ms	150ppm

SAINT-GOBAIN
CRYSTALS

Scintillation Products

SAINT-GOBAIN
CRYSTALS

USA

Saint-Gobain Crystals
12345 Kinsman Road
Newbury, OH 44065
Tel: (440) 564-2251
Fax: (440) 564-8047

Europe

Saint-Gobain Crystals
104 Route de Larchant
BP 521
77794 Nemours Cedex, France
Tel: 33 (1) 64 45 10 10
Fax: 33 (1) 64 45 10 01

P.O. Box 3093
3760 DB Soest
The Netherlands
Tel: 31 35 60 29 700
Fax: 31 35 60 29 214

Japan

Saint-Gobain KK, Crystals Division
3-7, Kojimachi, Chiyoda-ku,
Tokyo 102-0083 Japan
Tel: 81 (0) 3 3263 0559
Fax: 81 (0) 3 5212 2196

China

Saint-Gobain (China) Investment Co., Ltd.
15-01 CITIC Building
19 Jianguomenwai Ave.
Beijing 100004 China
Tel: 86 (0) 10 6513 0311
Fax: 86 (0) 10 6512 9843

www.detectors.saint-gobain.com

BGO
Bismuth Germanate Scintillation Material

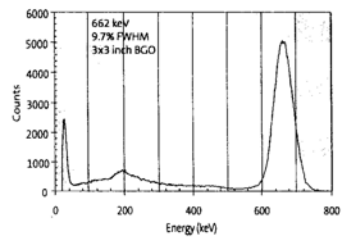

Figure 2. The pulse height spectrum of a 3" diameter, 3" high BGO crystal when irradiated with 662 keV γ-rays

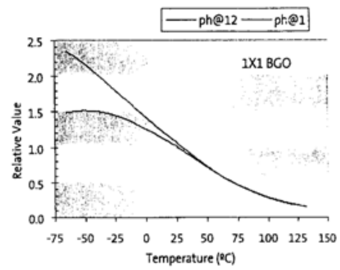

Figure 3. Temperature dependence of the scintillation light output of BGO (1μs and 12μs are the main amplifier shaping times)

The decay time of BGO is about 300ns at room temperature, which is comparable to that of NaI(Tl). As there is no slow component in BGO and the rise time is quite fast (intrinsic scintillator), it is possible to get good timing <2ns with 3" thick crystals.

The scintillation intensity of BGO is a strong function of the temperature. Figure 3 shows the relation. At room temperature, the rate of change with temperature is approximately -1.2%/C.

The radioactivity in BGO can make BGO unacceptable for some applications. We have developed a production process that significantly reduces the natural background, making our BGO well-suited for most applications.

BGO scintillation crystals are susceptible to radiation damage starting at radiation doses between 1 and 10 Gray (10^2 - 10^3 rad). The effect is largely reversible with time or annealing. Since the radiation damage to BGO crystals depends on the presence of sub ppm impurities, large differences between individual crystals can occur.

It is possible to read out BGO crystals with silicon photodiodes but, due to the moderate light output, this is only useful for the detection of high energy particles, or photons of more than a few MeV.

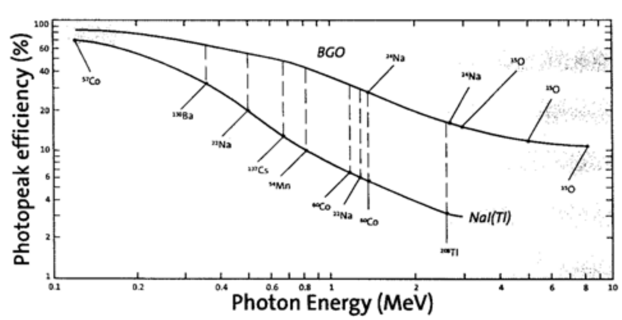

Figure 4. Photopeak efficiencies for BGO and NaI(Tl) scintillation detectors, 38mm diameter, 38 mm high.

(03-07)